Automated damage diagnostic system for laser damage threshold tests

Xiaofeng Liu (刘晓凤)[1,2*], Dawei Li (李大伟) [1], Yuan'an Zhao (赵元安)[1], Xiao Li (李 笑)[1,2], Xiulan Ling (凌秀兰)[1,2], and Jianda Shao (邵建达)[1]

[1]*Shanghai Institute of Optics and Fine Mechanics, Chinese Academy of Sciences, Shanghai 201800, China*

[2]*Graduate University of Chinese Academy of Sciences, Beijing 100049, China*

[*]*E-mail: xiaofeng198225@163.com*

Received August 17, 2009

An automated damage diagnostic system for collecting plasma flash is developed to diagnose damage in a laser-induced damage threshold (LIDT) test system. Experiment is done to verify the accuracy of this system and analyze the relationship between the plasma signals and the damage morphologies. The results obtained by the system are found to be in excellent agreement with those obtained by the much laborious method of Normaski microscope. Results show that plasma signals above 1 V correspond to the damage morphology of surface discolorations with or without pits in their centers, and plasma signals below or just around 1 V correspond to the damage morphology of pits. The misdiagnosis is attributed to contaminations and air breakdown.

OCIS codes: 140.3330, 310.0310.

doi: 10.3788/COL20100804.0407.

Laser-induced damage threshold (LIDT) is one of the most important standards to evaluate the performance of the optics. The exact LIDT test results not only provide scientific basis for coating process optimizations, but also provide safety guarantee for optical systems. Automated laser-damage test facilities, with different capabilities, have been set up in many laboratories[1−9]. The most striking differences of these facilities lie in their on-line damage diagnostic systems, and the damage diagnostic system is the key factor to determine the reliability of the test results. With further study on the damage characteristics of thin film optics and the development of large aperture components, previous on-line automated damage diagnostic methods encounter new challenges.

When irradiating a coated surface, especially a high reflector with silica protective layers which are widely used in high power laser systems, plasma could be created. The occurrence of plasma flash implies that irreversible changes appear in the test optics, and the optical element is damaged. It is said that these plasmas cause a scald or surface discoloration of the outer layer typically less than 10 nm deep[10]. Experiments show that such kind of damages cannot be easily and well detected by previous methods, such as optical microscopy (OM)[4], Raman microscopy[11], scanning electron microscopy (SEM)[12], atomic force microscopy (AFM)[13], photothermal microscopy[14,15], photothermal deflection[14], scatter detection[16−19], charge-coupled device (CCD) imaging[3], and so on. People used to observe plasma luminescence with eyes to identify such damages, but it is impractical for the large optics test, and moreover, human factors reduce the comparability of the test results.

Systems for measuring the effects of plasma scalding on beam modulation are introduced in Refs. [10,20], but automated damage diagnostic systems for collecting plasma flashes are seldom referred. In this letter, an automated real-time damage diagnostic system, reducing the testtime and removing the subjectivity of the human operator in damage threshold tests, is developed to detect plasma signals. The factors that influence on plasma detection are put forward and corresponding solutions are provided. Then results obtained by the method of the plasma detection are compared with those obtained via the much laborious method of Normaski microscope, and the relationship between damage morphologies and the intensity of the collected plasma signals is analyzed.

The LIDT test system is schematically shown in Fig. 1. The Q-switched Nd:YAG laser can be operated at three wavelengths, 1064, 532, and 355 nm. The output laser goes through a variable attenuator, and then is focused onto the target plane. The attenuator is comprised of a half-wave plate (HWP) and a polarizer. When rotating the HWP, the angle between the optical axis of the HWP and the polarization axis of the polarizer is changed, and it permits us to regulate the transferred laser energy from nearly zero up to the maximum available energy. A splitter wedge reflects two beams with reduced intensity: one is for the heat probe of digital power meter (EPM2000, Coherent Inc., USA) to monitor the laser energy, and the other is for the complementary metal oxide semiconductor (CMOS) probe of laser beam profiler

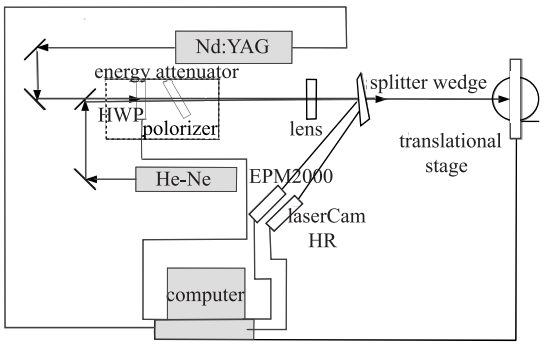

Fig. 1. Facility of the LIDT test.

(laserCam HR, Coherent Inc., USA) to monitor the laser profile. The probes of the above two laser diagnostic apparatuses are placed at the same optical distance from the splitter wedge as the sample. The laser beam is fixed in space, and the sample is moved by an X-Y translational stage, which can be rotated so that the coating can be tested at its used angle. An alignment He-Ne laser beam is made coaxially with the test laser beam after the attenuator.

If the sample is placed directly normal to the test beam, the damage diagnostic system must be angled to avoid being struck by the test beam. In our experiments, in order to collect the plasma signal effectively, laser irradiates the sample with a small incidence angle and the optical axis of the damage diagnostic system is normal to the sample.

The automated damage diagnostic system layout is shown in Fig. 2. When plasmas is generated, the lens collects the plasma luminescence and focuses the stray light onto a photodiode. The fast photodiode captures the light signal, which we call plasma flash because of its short duration, and changes it to a voltage signal called as plasma signal. The employed photo-detector is designed for detection of light signals over wavelength of 350 – 1100 nm. So the photodiode can respond to the test laser, whose wavelength is 1053 nm, and the He-Ne laser, whose wavelength is 632.8 nm. Plasmas may be created during the interaction of the laser with the coating. The voltage of the photodiode will increase because of the reflection and dispersion of the test laser. On the other hand, different scattering intensities of collimated laser on each test site will influence the voltage values in different degrees. Both of these factors make the transformed voltage signals have no comparability. So a high reflector is mounted before the collecting lens to block the reflection and the dispersion of the test laser and the He-Ne laser is closed after calibration. The Q switch signal sent to Nd:YAG laser by computer board and the plasma signal detected by the fast photodiode are shown in Fig. 3 . The rising of the plasma signal is quick and the relaxation is slow; strong plasma flash corresponds to a larger signal and weak plasma luminescence corresponds to a smaller signal; a peak exists in each collected plasma signal. The peak of the plasma signal always keeps a fixed delay time of nanosecond scale compared with the Q-switched signal, and keeps the value around peak for several microseconds, as shown in Fig. 4. In that case, we can capture the approximate peak in time. The circuit is designed to achieve this purpose. It tracks the plasma voltage signal and captures the signal peak. Computer records and compares this maximum value with the plasma signal threshold we set before test. If the value obtained exceeds the threshold, this site is recorded as a damage site. Because noises exist in the test environment, the circuit outputs some low noise voltages when no plasma flash appears. Before testing, we collect a series of noise signals to determine the maximum noise voltage value. The plasma signal threshold is set as the maximum noise voltage value.

The test system is automatically controlled. The spatial and temporal distributions of the laser are stable, and reducing time consumption is needed during measurement, so the laserCam HR is not incorporated into

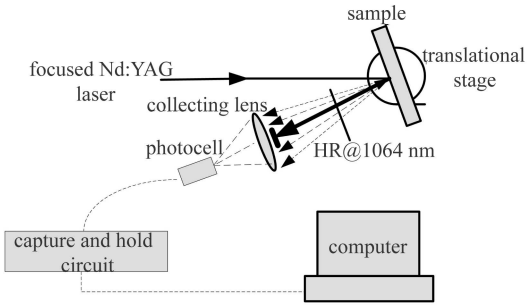

Fig. 2. Automated damage diagnostic system. HR: high reflection.

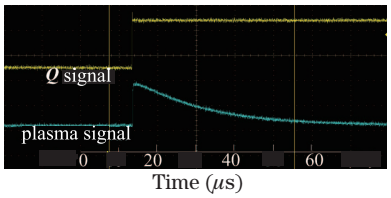

Fig. 3. Q switch signal and transformed voltage signal by plasma flashes.

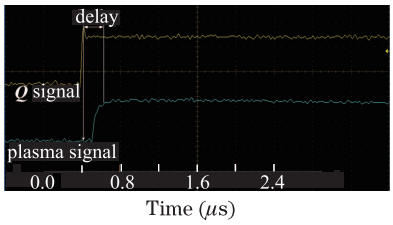

Fig. 4. Local enlarged view of the signals in Fig. 3.

our software. The automated damage diagnostic system presented in this letter is implemented to identify the damage. The software controls the output of the laser, the rotation of the HWP, the intensity of the irradiating laser, the acquisition and comparison of the damage diagnostic signals, and the motion of the sample stage. The sample is raster scanned, as shown in Fig. 5. Two hundred test sites, each of which is irradiated with only one shot, were tested and ten different energy steps were chosen in our experiment. The computer reads the plasma signal peak from the circuit after every irradiation. The collected noise signals are shown in Fig. 6, whose vlotages are almost under 0.07 V, so the plasma signal threshold was set as 0.07 V in our test environment.

The automated acquisition process of the plasma signal peak in the test of each site takes up only 10 ms, which improves the efficiency of our test and reduces unfavorable factors of the test accuracy.

According to the collected plasma signal peaks shown in Fig. 7, 116 sites are diagnosed to be damaged and 84 sites are not damaged. When observing the test sample under Normarski microscope, damages derived from the automated damage diagnostic system are found to be in excellent agreement with those obtained by Normarski post damage analysis. It is found that only three sites in two hundred, which are the 113rd, 140th, and 172nd,

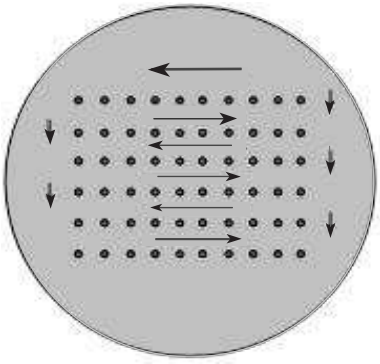

Fig. 5. Raster scan on the sample.

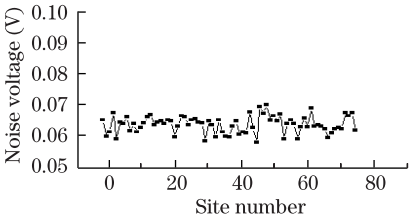

Fig. 6. Noise signal values before the LIDT test.

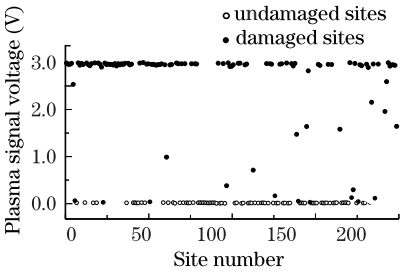

Fig. 7. Recorded plasma signal peaks in the test process.

are not consisted with the automated diagnostic results. The collected plasma signals of these three sites are 0.719, 0.0971, and 0.167 V. For other sites, the automated diagnostic result is in complete agreement with that obtained by Normaski microscope.

The most common damage morphology identified by plasma luminescence detection is the surface discoloration without or with a central pit in it, as shown in Fig. 8. When checking the collected plasma signals of all these sites, it is found that all the signal peaks exceed 1 V. Plasma flashes can be considered as a symbol of surface discoloration damage to a certain extent when the plasma signal peak exceed 1 V. Small signals below 1 V or just around 1 V correspond with small pits without surface discolorations, as shown in Fig. 9. Because of the limited resolution of the microscope, some pits are hard to identify whether they are damaged or exist before laser irradiation. In order to further verify the results, we offer the SEM pictures of these sites in Fig. 9. These small pits are similar to the pits in surface discolorations. The phenomenon implies that small signals correspond to small pit damages, and only when the plasma flashes are strong enough that the surface discolorations can be induced.

For the site, the damage is identified by the automated diagnostic system presented in this letter, but is not

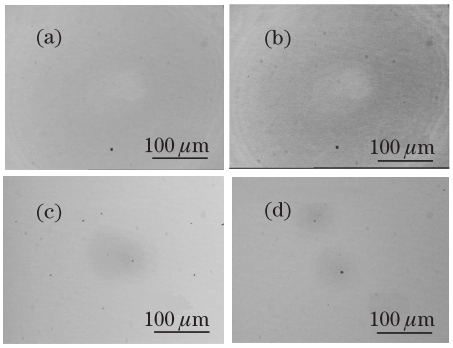

Fig. 8. Typical damage morphologies when the collected signal peaks are above 1 V. Plasma signal voltages are (a) 2.8499 V; (b) 2.8554 V; (c) 1.597 V; (d)1.4421 V.

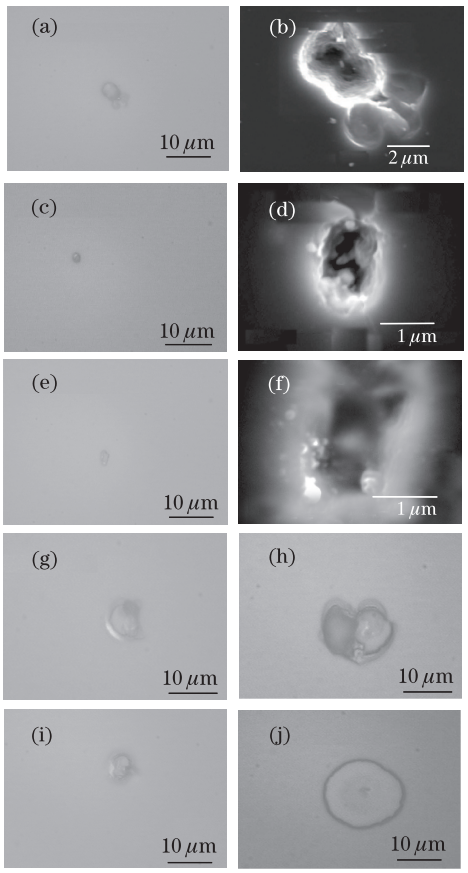

Fig. 9. Typical damage morphologies when the collected signal peaks are below or just around 1 V. Plasma signal voltages are (a), (b) 0.1553 V; (c), (d) 0.4062 V; (e), (f) 0.2037 V; (g) 0.9809 V; (h) 0.1065 V; (i) 0.0861 V; (j) 0.0761 V. (b), (d), and (f) are the SEM pictures.

identified by Normaski microscope. One possible reason can be responsible for this case. It is pointed out that contamination and air breakdown can also create plasma flashes[21]. Clean environment can reduce contaminations and air breakdown, but they are not completely avoided, and sometimes damage is not induced if plasmas are created by contaminations and air breakdown.

In conclusion, an automated damage diagnostic system reducing time and labour demands is developed. The experimental result shows that the automated damage diagnostic system is an effective method to identify

damage automatically, and there is a good agreement between the results obtained from the automated damage diagnostic system and the Normaski microscope. Larger signals always correspond to the surface discoloration damage and smaller signals always correspond to pits without surface discoloration. Contamination and air breakdown, which cannot be completely avoided in each LIDT test, should be responsible for the misdiagnosis.

This work was supported by the National High Technology Research and Development Program of China under Grant No. 2006AA804908.

References

1. D. Li, Y. Zhao, J. Shao, Z. Fan, and H. He, Chin. Opt. Lett. **6**, 386 (2008).
2. M. E. Innocenzi, M. Bass, and H. Deng, Appl. Opt. **25**, 658 (1986).
3. X. Liu, D. Li, X. Li, Y. Zhao, and J. Shao, Chinese J. Lasers (in Chinese) **36,** 1545 (2009).
4. J. Hu, L. Yang, F. Qiu, X. Zeng, and F. Yang, Proc. SPIE **4231,** 352 (2000).
5. H. Jean, D. Jean, and L. Philippe, Proc. SPIE **2714,** 102 (1996).
6. M. Josse, R. Courchinoux, L. Lamaignere, J. C. Poncetta, T. Donval, and H. Bercegol, Proc. SPIE **5647,** 365 (2005).
7. L. M. Sheeham, M. R. Kozlowski, F. Rainer, and M. C. Staggs, Proc. SPIE **2714,** 559 (1993).
8. L. Sheehan, S. Schwartz, C. Battersby, R. Dickson, R. Jennings, J. Kimmons, M. Kozlowski, S. Maricle, R. Mouser, M. Runkel, and C. Weinzapfel, Proc. SPIE **3578,** 302 (1999).
9. M. R. Borden, J. A. Folta, C. J. Stolz, J. R. Taylor, J. E. Wolfe, A. J. Griffin, and M. D. Thomas, Proc. SPIE **5991,** 59912A (2005).
10. J. R. Schmidt, M. J. Runkel, K. E. Martin, and C. J. Stolz, Proc. SPIE **6720,** 67201H (2008).
11. P. M. Fauchet and I. H. Campbell, Damage in Laser Materials **746,** 388 (1985).
12. M. Poulingue, J. Dijon, P. Garrec, and P. Lyan, Proc. SPIE **3578,** 188 (1999).
13. M. R. Kozlowski, M. Staggs, M. Balooch, R. Tench, and W. Siekhaus, Proc. SPIE **1556,** 68 (1992).
14. C. Tao, Y. Zhao, H. He, D. Li, J. Shao, and Z. Fan, Chin. Opt. Lett. **7,** 1061 (2009)
15. B. Bertussi, J. Y. Natoli, and M. Commandre, Proc. SPIE **5647,** 394 (2005).
16. L. C. Malacarne, F. Sato, P. R. B. Pedreira, A. C. Bento, R. S. Mendes, M. L. Baesso, N. G. C. Astrath, and J. Shen, Appl. Phy. Lett. **92,** 131903 (2008).
17. L. Sheehan, M. Kozlowski, and F. Rainer, Proc. SPIE **2428,** 13 (1995).
18. J. B. Franck, S. C. Seitel, V. A. Hodgkin, W. N. Faith, and J. N. Porteus, in *Proceedings of Sixteenth Annual Symposium on Optical Material for High Power Lasers* 71 (1984).
19. N. C. Kerr and D. C. Emmony, J. Mod. Opt. **37,** 787 (1990).
20. L. Laurent, V. Cavarro, C. A. D. Bernardino, M. Josse, and H. Bercegol, Proc. SPIE **4679,** 410 (2002).
21. F. Y. Genin and C. J. Stolz, Proc. SPIE **2870,** 439 (1996).